Available online at www.sciencedirect.com
ScienceDirect
Cement and Concrete Research 37 (2007) 337–347
Cement and Concrete Research

Molecular dynamics modeling of the structure, dynamics and energetics of mineral–water interfaces: Application to cement materials

Andrey G. Kalinichev [a,b], Jianwei Wang [a,1], R. James Kirkpatrick [a,b,*]

[a] Department of Geology, University of Illinois at Urbana-Champaign, Urbana, IL 61801, USA
[b] ACBM Center, University of Illinois at Urbana-Champaign, Urbana, IL 61801, USA

Received 7 October 2005; accepted 13 July 2006

Abstract

This paper reviews molecular modeling studies of water structure in nano-confinement and at fluid–solid interfaces and presents new molecular dynamics (MD) modeling results for water on the surface of tobermorite. MD modeling provides detailed information about the structure, dynamics and energetics of water at solid surfaces and in confinement that can add significant additional molecular scale insight to experimental results. For the tobermorite (001) surface the results show strong structuring of water in the channels between the drietkette silicate chains and above the surface due to the development of an integrated H-bond network involving the water and the surface sites. Calculated diffusion coefficients for the surface-associated water are in good agreement with published experimental results.

Keywords: Molecular dynamics modeling; Tobermorite; C–S–H; Pore solution; Pores

1. Introduction

Hydrated cements have pore sizes that range from a few nanometers to microns, and the physical and chemical properties of cements, including strength, shrinkage, creep, and chemical reactivity are greatly influenced by water and solute in the pore system. A major challenge to cement science is to understand the behavior of this water on different length and time scales, to understand the molecular scale origin of its behavior, and to be able to control the physical and chemical properties of cement-based materials by tailoring the characteristics of the pore system. It has long been known that the structure and physical properties of water near surfaces can be substantially different than those of bulk water, that surfaces can perturb the fluid structure and properties up to several molecular diameters from the surface, and that these differences are key to understanding mineral surface chemistry. Despite decades of study, however, the structure, dynamics and physical properties of this near-surface water remains incompletely understood [1–28]. For cement materials, recent experimental studies involving especially field cycling NMR relaxation and neutron scattering methods are adding significant new insight [29–33].

Computational modeling using both quantum chemical methods and force-field based, molecular-scale methods including molecular dynamics (MD) and Monte Carlo (MC) techniques offers significant, untapped potential to investigate water and its interaction with solid surfaces in cement systems. Molecular computer simulation is playing an important role in advancing understanding of near-surface water for many kinds of materials [5–8,11–13,27,28,34–42]. Here we review the results of recent computational MD modeling that provide new insight into the structure, dynamics, energetics of water and solute on the surfaces oxide and hydroxide phases and in confined spaces. Key points from these results are the following. (1) The development of an integrated, 3-dimensional hydrogen-bonding (H-bond) network across and perpendicular to the surface plays a dominant role in controlling the properties. (2) The structure of this H-bond network is greatly influenced by the substrate structure, composition and charge distribution. (3) The evaluation of molecular-scale

* Corresponding author. Department of Geology, University of Illinois at Urbana-Champaign, Urbana, IL 61801, USA.
E-mail address: kirkpat@uiuc.edu (R.J. Kirkpatrick).
[1] Current address: Department of Geology, University of California at Davis, Davis, CA 95616, USA.

0008-8846/$ - see front matter © 2006 Elsevier Ltd. All rights reserved.
doi:10.1016/j.cemconres.2006.07.004

dynamical effects is essential to understanding these interactions and the structure and properties of surface-associated water cannot be understood independently of dynamical behavior over a wide range of frequencies.

MD computer simulations provide an effective method to quantitatively investigate the statistical properties of H-bond networks, because relative to quantum chemical methods the useable system sizes are significantly larger and the simulation durations can be significantly longer (e.g., [43,44]), and because well-tested potentials are readily available (e.g., [45,46]). Several papers in the volume "Molecular Modeling Theory and Application in the Geosciences" [47] discuss important aspects of molecular modeling theory and methods as applied to aqueous solutions and mineral–solution interfaces, and Kirkpatrick et al. [48] discuss the details of calculating vibrational dynamics of surface and interlayer species.

Application of computational molecular modeling techniques in cement and concrete science has increased rapidly in recent years. There have been a number of studies of the origin of the cohesion forces in hydrated cement paste or applying the results [49–58]. There have also been studies of the structure of C–S–H [59], the origin of the effect of borate and phosphonate retarders [60,61], the structure of AFm phases [12], Cl^- binding in hydrated cement pastes [40,62], and the structure of model ASR phases [63].

2. Molecular dynamics simulations

The theory of classical MD simulations and the computational algorithms needed to effectively implement these methods on large, multi-processor computers are well developed (e.g., [64]). The key issue for a given class of problems is the set of interatomic potentials (the force field) used for the calculations, and their many different approaches. We employ the *CLAYFF* force field [46], which is specifically optimized for low-temperature hydrous minerals and does not require a priori definition of most chemical bonds. With the current generation of computers, this non-bonded (pseudo-ionic) approach allows the study of large, complex and disordered systems containing hundreds of thousands of atoms in solid and fluid phases and at solid–fluid interfaces. It is intrinsically less accurate than ab initio and quantum MD methods, but it is able to capture the complex and cooperative interactions that are critical to understand interfacial and nano-confined water. The absence of defined chemical bonds for most interatomic interactions allows effective and relatively simple treatment of solids, fluids and interfaces and proper accounting of energy and momentum transfer between the fluid phase and the solid. It also keeps the number of interaction parameters small enough to allow modeling of large and highly disordered systems. The only defined bonds in *CLAYFF* are O–H in H_2O, OH-groups in the solid and on the solid surface, and the bonds in aqueous oxyanions (e.g., SO_4^{-2}). The flexible simple point charge (SPC) water model [65,66] is used to describe the H_2O and OH behavior. This model has been well tested in many simulations of aqueous systems (e.g., [45,67–69]). The principal limitation of this approach is that it does not allow for ligand exchange reactions such as making and breaking of O–H bonds, thus preventing modeling of proton exchange reactions in the fluid or with the surface. This imitation requires a priori definition of the surface protonation state to model, e.g., pH dependent behavior. Development of generally applicable reactive force fields capable of addressing these situations is a significant need in cement chemistry [41,70–72]. Cygan et al. [46], Kalinichev and Kirkpatrick [40], and Kirkpatrick et al. [48,63] show examples that demonstrate the effectiveness of the *CLAYFF* approach, and Kirkpatrick et al. [73] provides additional discussion of the wide range of different modeling approaches now in use.

MD simulations are performed by building the desired computer model of the structure, assigning the individual atoms or molecules initial positions and velocities, and then allowing

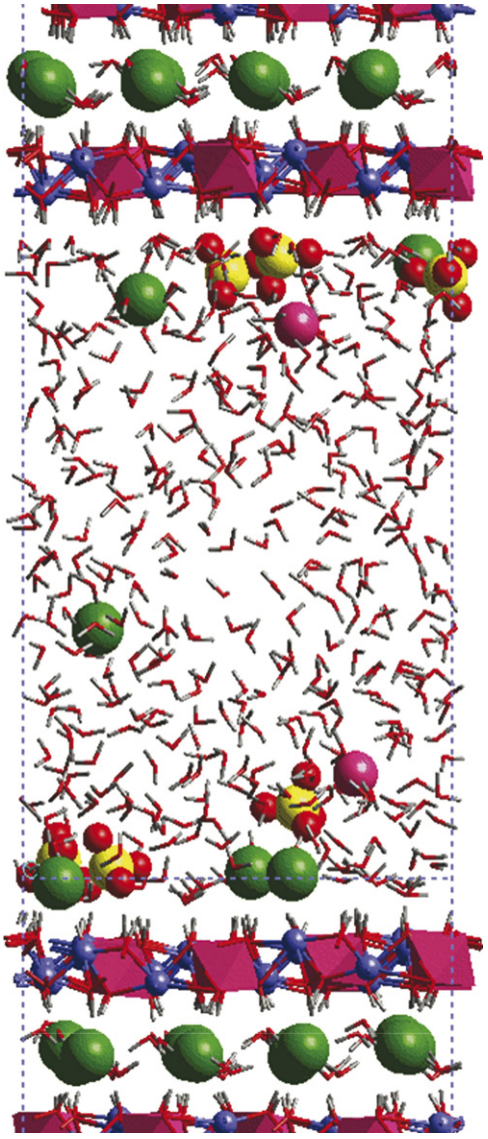

Fig. 1. A typical MD simulation cell used in the modeling of mineral–solution interfaces. The top and bottom crystal structures are Friedel's salt, and the central region is water containing Cl^-, SO_4^{2-}, and Na^+. The aqueous layer is approximately 30 Å thick in this model. (Colour is clearly a critical element of the techniques used in this study, so the text and images of this paper have not been modified, despite the fact that images in Cement and Concrete Research are printed in black and white. A full colour copy of this paper is available online at http://www.sciencedirect.com/.)

the system to evolve according to the laws of classical Newtonian mechanics and the imposed interatomic interaction potentials (force field). These structures can be built atom-by-atom, but for crystalline phases they are more typically based on the positional parameters of known structures. These structures can be modified as needed to, for instance, account for positional disorder over a crystallographic site or to protonate or deprotonate a particular surface O-atom or OH-group. Three-dimensional periodic boundary conditions are typically applied to model a bulk system, and Ewald summation is used to account for long-range Coulombic interactions (e.g., [64]). Models of mineral–fluid interfaces are generated by cleaving the mineral model structures, often in the middle of an interlayer, and filling all or part of the remainder of the simulation box with water molecules or aqueous solution (Fig. 1). In most cases, the number of H_2O molecules in this layer is chosen to give a fluid density of ~1 g/cm^3. In our simulations, the thickness of the water layer is typically more than 30 Å to minimize interaction of one surface with another in the periodic model structure. The structural and dynamical effects of surfaces extend to about 15 Å (approximately five diameters of a water molecule), and with water layers greater than 30 Å thick, the water in the center of the layer has essentially bulk liquid properties, and the water at one interface is not affected by the opposite interface to any significant extent (e.g., [42]). The time step for the numerical integration of the Newtonian equations of motion for the system of N atoms is, typically, 0.001 ps, and the resulting dynamic trajectory of the simulated system in its *phase space* (an ideal multi-dimensional space in which the 6 N coordinate dimensions represent the positions and velocities of all N atoms) is recorded for analysis every 0.004 ps. As in all computational approaches to molecular scale problems, care must be taken to adequately sample the phase space of the system to ensure that it is not trapped in a local energy minimum. For crystalline phases this is not usually a difficult problem, because the starting configuration is normally a known structure. For aqueous fluids and solid–fluid interfaces without solute, the reorientational and diffusional correlation times of water molecules are relatively short, and the system properties typically converge to their equilibrium values over a few 10 s of ps. For systems containing a solid-fluid interface and dissolved solute, we position the ions in the aqueous phase at distances not less than 8–10 Å (~3 molecular diameters of H_2O) from the solid surface and carefully monitor their dynamic evolution and any adsorption onto the surface.

A typical simulation normally consists of a pre-equilibration stage in which the atoms move under only an energy minimization algorithm, a further pre-equilibration period of MD simulation lasting 50–500 ps during which the system reaches its equilibrium thermodynamic state, and a final equilibrium MD period of typically 100 ps to 1000 ps during which the trajectories of all atoms are recorded for further statistical analysis. For solid–fluid systems containing solute species, those atoms that become associated with the interface typically move to it during the pre-equilibration stage but often undergo exchange with the solution during the MD runs. This allows evaluation of surface site lifetimes. Quantitative results for structural parameters such as radial distribution functions (RDFs), interatomic distances and angles, and H-bond configurations; dynamic parameters such as diffusion coefficients, adsorption site lifetimes, and power spectra of atomic motion; and energetic parameters such as bulk system energy and energies of adsorption are obtained only from analysis of the equilibrium stage of the MD trajectories. The power spectra (total dynamical density of states) of the entire system, individual species and even the motion of individual species in particular directions are calculated by Fourier transformation of the atomic velocity autocorrelation functions (e.g., [48]).

Hydrogen bonding plays a dominant role in defining water structure and dynamics, and detailed analysis of the H-bond network in the simulated system is important in understanding its structure, dynamics and energetics. The criteria for the existence of a –O···H–O hydrogen bond (HB) used here are those often used for bulk liquid water [74]: the intermolecular O···H distance ($R_{O\cdots H}$) less than 2.45 Å and the angle, β, between the O–H vector in the H-bond donor group and the O···O vector connecting the H-bond donor and acceptor molecules of less than 30°. Surface O–H groups are treated in the same way as O–H of water molecules for the purpose of HB calculations. The threshold of $R_{O\cdots H} \leq 2.45$ Å is used because it corresponds to the first minimum in the O–H radial distribution function for SPC water at ambient conditions, and $\beta \leq 30°$ includes 90% of the angular distribution of H-bonds in water under the same conditions [74,75].

3. Results and discussion

3.1. Hydroxide phases

Most hydrated phases in cement paste, including C–S–H, portlandite ($Ca(OH)_2$), AFm phases and AFt phases, are either hydroxides or expose hydroxyl groups to the pore fluid [76,77]. Thus, understanding water and solute species at hydroxylated surfaces is critical to understanding cement paste on the molecular scale. We have undertaken studies of water on the charge-neutral phases portlandite, brucite ($Mg(OH)_2$), and gibbsite ($Al(OH)_3$) and on the positively charged layered double hydroxides (LDHs), including hydrotalcite and the Cl^- AFm phase Friedel's salt. LDH phases develop permanent, positive structural charge due to aliovalent cation substitution in the hydroxide sheets, and the interfacial water structure on them is significantly different than for neutral hydroxides due to Coulombic attraction of the negatively charged O-atom of the water molecules to the positive structural charge of the double hydroxides [78].

Solid surfaces can perturb the water structure and dynamics by affecting its molecular packing, orientation, rotation and translation. These effects arise due to the excluded volume effect, the presence of electrostatic fields, and local surface-specific H-bonding donor and acceptor sites (e.g., [21,40–43,79]). The excluded volume ("hard wall") effect creates near-surface layering due to the spatial geometric constraint that atoms or molecules at the surface cannot penetrate it, analogous to cement particles packing next to an aggregate grain. This effect occurs for all confined fluids [80]. Thus, the structure of water in an interfacial region reflects a delicate balance of the ordering due to excluded volume effects on the packing of H_2O molecules, surface-specific

H-bonding and orientational ordering of the water molecules, and disordering due to thermal motion. This structure is typically different and more disordered than the tetrahedral, H-bonded structure of ice Ih, which is still prominently present in the more disordered short-range tetrahedral H-bonding molecular arrangements in bulk liquid water (e.g, [67–69,81–83]).

For hydrophilic phases such as hydroxides, H-bonding between the surface and water molecules and among water molecules both play central roles, whereas for hydrophobic phases such as carbon nano-tubes and talc, H-bonding among the water molecules is important, but the interaction between the surface and water is much less significant. Many studies of surface-water structure rely on computed profiles of atomic density variations with distance from the surface, comparable to radial distribution functions, sometimes supplemented by profiles of molecular H_2O orientation. We have found that computed statistics for molecular nearest neighbor coordination, H-bonding, and order parameters related to the local structural arrangements in the fluid [83,84] provide important additional information that leads to a greatly improved, atomistically detailed understanding [12,40,42,62,63,73,79,85].

The MD results for water at the portlandite, brucite, and gibbsite surfaces show that these hydrophilic substrates significantly influence the near-surface water structure, with both H-bond donation to the surface oxygen atoms and H-bond acceptance from the surface hydrogen atoms in the first surface layer of H_2O molecules playing key roles [40,42,85]. The local O and H atomic densities deviate from those of bulk water to distances as large as 10 Å (Fig. 2). The distances between maxima in the O-density profiles are not equally spaced, as would be expected from the molecular spacing effects of excluded volume alone, clearly demonstrating that surface structure, charge distribution and H-bonding play important roles in controlling the near-surface water structure. The H_2O dipole orientations show structuring to as far as 15 Å (~5 molecular water layers) from the surface. The average number of H-bonds per H_2O molecule changes from 3.8 in the near-surface layer to 3.5 (approximately the value for bulk SPC water) at ~10 Å from the surface, and there are significant oscillations in this value closer to the surface.

Confinement of water in the approximately 5 nm (50 Å) pores in C–S–H gel plays a critical but poorly understood role in controlling its properties, and recent results indicate that confinement of water and solute (Ca^{2+}) between C–S–H particles is critical to the cohesion that controls the strength of cement paste [49–58]. MD simulations for water in nanometer-scale confinement in slit-like pores bounded by $Mg(OH)_2$ (001) surfaces show significant overlap of the structural effects of the two surfaces for pores less than at least 15 Å thick (Fig. 2) [42]. For thin pores, the structure of the entire water volume is substantially perturbed compared to bulk water, and the effects of the surface depend significantly on pore thickness.

For the unconfined brucite surface, the variation in atomic density reflects the presence of three important, well-defined layers. These are a high atomic density, highly structured, near-surface layer centered near 2.5 Å that contains molecules that are directly coordinated to the surface, a transitional layer centered near 4.0 Å from the surface with a lower atomic density, and a region extending from about 5 Å to 15 Å from the surface in which the structure becomes progressively more similar to that of bulk water. Fig. 3 illustrates schematically the most common orientations of water molecules in these layers close to an electrostatically neutral hydroxide surface. As an example of the structural insight for disordered systems that can be obtained from MD simulations, we describe the results for brucite in some detail.

The layer nearest the surface contains two principal types of water molecules, both of which are directly coordinated to surface OH groups. One type is on average slightly closer to the surface (mean distance ~2.3 Å) and is oriented predominantly with the positive (hydrogen) end of their molecular dipoles towards the surface, making an average angle of ~130° with the surface normal. These molecules typically have nearest neighbor (NN) coordinations of six, three surface OH groups and three H_2O. On average, they accept ~0.5 H-bonds from surface OH groups, donate 1.0 H-bond to surface OH groups, accept ~1.3 H-bonds from other water molecules, and donate ~0.8 H-bonds to other water molecules. The second type is on average ~2.6 Å from the surface and is oriented predominantly with the positive ends of their dipoles pointing away from the

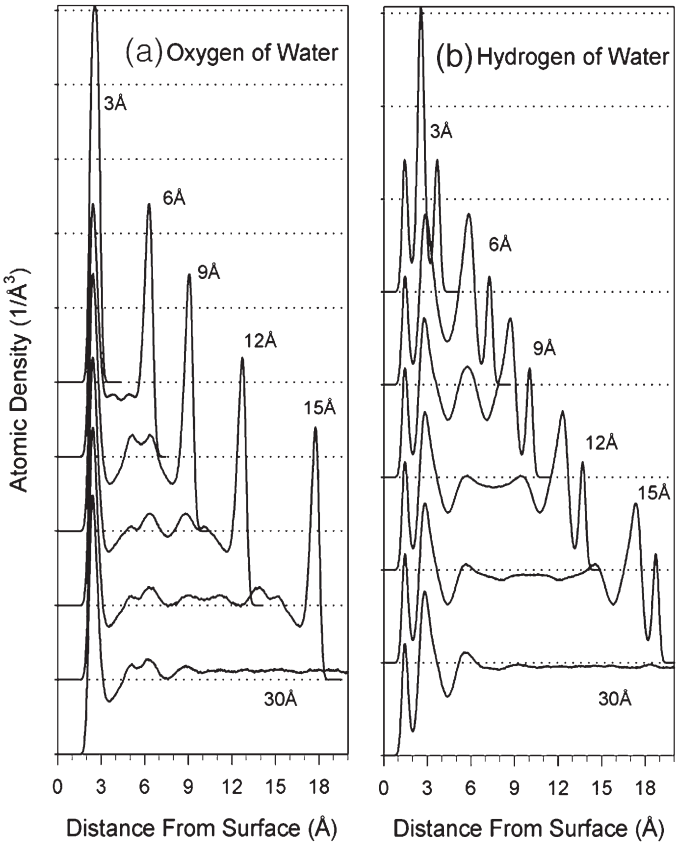

Fig. 2. Computed atomic density profiles for water confined between brucite layers. Curves are displaced vertically by 0.03 $Å^{-3}$ (oxygen atomic density) and 0.07 $Å^{-3}$ (hydrogen atomic density) to avoid overlap. The position of the surface (0.0 in these plots) is computed as the average position of the brucite surface oxygen atoms. The system size labels are the increases of the brucite *c*-axis dimension used to generate the systems. The actual water layer thicknesses vary somewhat from these values.

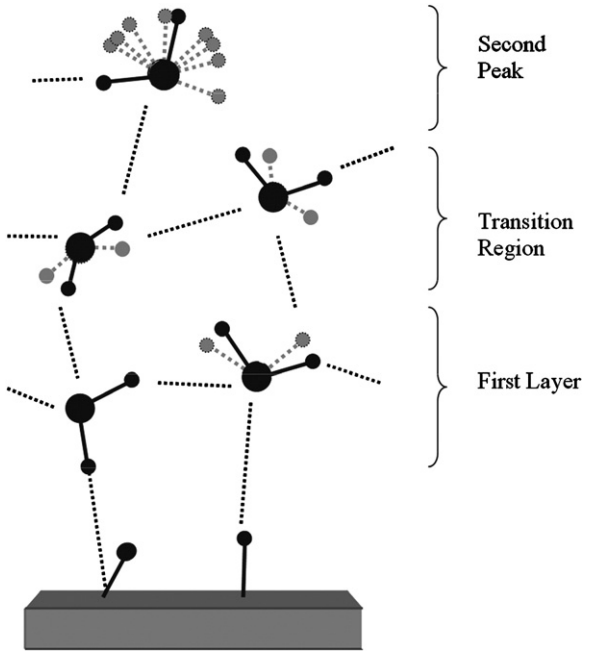

Fig. 3. Schematic diagram illustrating the orientations and H-bonding of water molecules in the different near-surface layers for a hydroxide mineral surface. Black balls and sticks are water molecules or surface OH groups. Dotted balls and sticks are water molecules with different orientations, which schematically show the orientational ranges in the different layers. The dotted lines connecting water molecules are H-bonds.

surface, making angles of ~30–80° with the surface normal. These molecules typically have NN coordinations of five, one surface OH-group and four water molecules. On average, they accept ~0.5 H-bonds from surface OH-groups, donate none to surface OH groups, accept ~1.4 H-bonds to other water molecules and donate ~1.7 H-bonds to other water molecules. The (type 1)/(type 2) abundance ratio is about 5:4. The two types are intimately mixed with each other in the plane parallel to the surface. Large domains of one structural type cannot form, because H-bond formation between neighboring water molecules prevents each type of environment from extending more than 3 molecules in the plane parallel to the surface.

These two types of H_2O occur on very different surface sites. The first type is preferentially located above the vacant tetrahedral sites of the trioctahedral sheet and forms a reasonably well-ordered and dynamically averaged 2-dimensional hexagonal network that reflects the underlying brucite structure. There are four local potential energy minima on which they occur. One of these is at the center of the OH-triangle, and three are near the middle of the line connecting two nearest neighbor OH sites. The water molecules spend on average about 1/2 of the time at the OH-triangle center, where they accept 1 HB, and 1/6 of the time at each of the other sites, where they donate 1 and accept 1 HB. This site hopping, libration, and formation and breaking of HBs result in the computed average of 1.5 HBs with surface OH groups. The second type of water molecule is preferentially located above the surface OH groups, and their distribution is much less ordered than for the first. Only half of them accept one H-bond from surface OH groups at any instant.

Further from the surface, the low-density region between 3 Å and 5 Å from the surface provides the essential transition between the near-surface layer, with a structure largely controlled by the substrate surface, to a structure more or less like bulk water (Fig. 3). This transition occurs by gradual adjustment of the second neighbor configuration in a distorted, but locally tetrahedrally coordinated structure. The NN coordination in this region is about 4.4, similar to that of bulk liquid water at the same temperature and density. Molecules in this region have two different preferred orientations, and as in the first layer, these types are mixed on a molecular scale across the surface. The orientational order is, however, much less than in the first layer. Type 3 molecules have their positive ends generally oriented towards the surface, making angles between 90 and 180° with the surface normal. Type 4 molecules have their positive ends generally oriented away from the surface, making angles between 40 and 140° with the surface normal. The (type 3)/(type 4) abundance ratio varies from 2:1 at 3 Å from the surface, to 4:1 at 4 Å, and back to 2:1 at about 5 Å.

The greatest degree of the tetrahedral (ice-like) molecular ordering in the interfacial region occurs at about 4 Å from the surface, where the O-density has its minimum value. At this distance, the water molecules are locally more ordered (more similar to ice Ih) than in bulk liquid water. Such structuring is in agreement with the notion that the number of water molecules with four H-bonds increases with decreasing density at liquid-like densities [68,86,87]. Similar structuring is also observed for water confined in pores in hydroxylated silica glass [39].

Beyond about 6 Å from the surface, the water structure is generally similar to that of bulk liquid [67–69], with an average of about 3.5 H-bonds per molecule and an average NN coordination of about 4.5. The atomic density profiles show statistically meaningful variation to ~10 Å from the surface, and small but statistically meaningful variations in the molecular orientations occur out to about 15 Å from the surface. These changes of angular distribution are due to adjustment of the orientations of individual water molecules to fit their local environments, which are perturbed indirectly by the surface through its effects on H_2O molecules next to it.

The water structure in the layer closest to the brucite surface does not resemble those of ice Ih, bulk water at ambient conditions, or water at low temperatures, as has been proposed for water confined in Vycor glass and silica gel based on neutron diffraction studies [14,23]. This is shown by the 5- and 6-fold NN coordinations of the near-surface molecules and by this coordination being as much as 2.2 times larger than the H-bond number. In ice Ih, the NN coordination and H-bond number are both about 4.0 [82], and in bulk SPC liquid water at ambient temperature and pressure the NN coordination is about 4.4 and the H-bond number is about 3.5. Cooling of bulk liquid water causes the average number of H-bonds to increase with the NN coordination remaining more or less constant [87,88].

The structure of the first layer of water does share some similarities with those of high-pressure ice phases and liquid water at elevated pressure. With increasing pressure, the average NN coordination for liquid water increases more rapidly than the average number of H-bonds [36,87], and the structural changes can best be interpreted in terms of an increasing number of

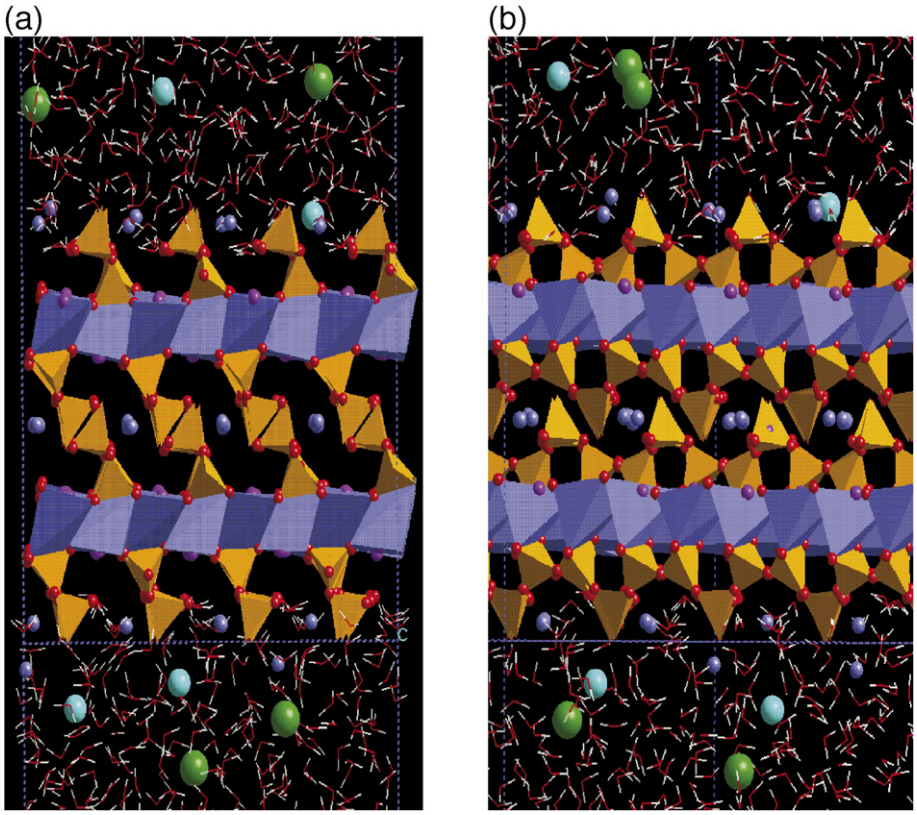

Fig. 4. The simulation cell used for 9 Å tobermorite. (a) Looking down the drierkette chains. (b) Looking perpendicular to the drierkette chains.

interstitial (non-H-bonded) water molecules in the NN coordination sphere [36,89,90]. In the crystalline ice phases, there are always four H-bonded nearest neighbors at intermolecular distances of 2.7–2.9 Å, but the number and intermolecular distances of the non-H-bonded molecules are different for different phases. There are zero non-H-bonded molecules in ice Ih (stable up to 0.3 GPa), 3.75 at 3.1–3.3 Å in ice IV (a metastable phase at 0.4–0.55 GPa, [91]), and 4 at 2.74 Å in ice VIII (stable above 2.1 GPa, [92]). The latter distance is shorter than the H-bond distance (2.88 Å) in that phase, paralleling a similar trend for liquid water under pressure [93]. At the brucite surface, the coordination number of type 1 molecules is 6 and number of H-bonds is about 3.8, qualitatively following the trends for liquid water and the crystalline phases with increasing pressure.

The MD modeling for water at the brucite surface adds to a growing body of computational and experimental studies that demonstrate that different types of surfaces can have substantially different effects on surface water structure and that this structure should not be thought of as simply "ice-like". For instance, previously published MD simulations for water at a variety of oxide and hydroxide surfaces show the presence of molecules with two different and well-defined orientations in the first layer and that the local structural environments or orientations are different for different phases. The coexistence of water molecules with different orientations mixed and interconnected in the plane parallel to the surface appears to allow the development of an interconnected H-bond network involving the water molecules and surface atoms. The interfacial water on the portlandite, $Ca(OH)_2$, (001) surface is similar to that for brucite due to the similarity in their structures and involves H-bond donation and acceptance to/from the solid surface [40]. MD simulations for water at the magnetite (001) surface using a potential model that allows the surface protonation state to change during the MD simulation show that H-bond donation and acceptance between the surface and H_2O are important in this situation also [41]. On this surface, interfacial water molecules accept H-bonds from several surface functional groups, of which about 50% are $^{[6]}FeOH_2$ sites (doubly protonated O-atoms coordinated to one octahedral Fe). About 75% of the H-bonds donated by H_2O molecules to surface sites go to $^{[4]}FeOH$ (singly protonated O-atoms coordinated to tetrahedral Fe). These results suggest that different surface functional groups can play different roles in developing interfacial H-bonding networks. In contrast, our model portlandite and brucite (001) surfaces contain only one type of surface functional group ($^{[6]}M_3OH$) that serves as both an H-bond donor and acceptor.

Lee and Rossky [34] have proposed two idealized H-bond structures for water in the first hydration layer of a hydroxylated silica surface, and these are quite different from those for brucite. One type has the positive end of its dipole oriented away from the surface and accepts one H-bond from and donates one H-bond to surface OH groups. The other type has the positive end of its dipole oriented towards the surface and accepts one H-bond from and donates two H-bonds to surface OH groups. The differences between water orientations at the brucite and hydroxylated silica surfaces appear to be caused by the differences in the substrate surface structure. On the silica surface modeled by Lee and Rossky, the Si–OH groups are

5.0 Å apart, whereas for brucite the nearest MgOH–MgOH distance is only 3.1 Å, approximately the diameter of a water molecule. MD simulations for water confined in pores in hydrated Vycor glass show that the ice Ih-like NN and H-bond geometry of bulk water is destroyed near these surfaces [39]. MD simulations of water at the NaCl (100) surface show a lattice-like 2-D distribution of water molecules parallel to the surface [8], and as for portlandite and brucite this 2-D structure reflects the underlying NaCl crystal structure.

The presence of both donating and accepting H-bond configurations at hydroxylated surfaces is not universal. H_2O molecules on the surface of hydrotalcite, Friedel's salt, and presumably other AFm phases, have the positive ends (H-atoms) of their dipoles pointing only away from the surface due to the positive structural layer charge of these phases. These waters accept H-bonds from the surface OH-groups but do not donate any to them [40,85]. For Friedel's salt, the MD results demonstrate that the structural environments of water and Cl^- on the basal surface are similar in some ways to those in the interlayer but are more disordered both statically and dynamically [12,40]. Surface Cl^- are associated with the surface principally as inner sphere complexes due to their large electrostatic interaction with the hydroxide sheets. In contrast to the highly ordered interlayer, however, the Cl^- and H_2O are disordered over sites comparable to the "Cl^-" and "H_2O" sites in the interlayer. The "H_2O" site is directly coordinated to Ca, whereas the "Cl^-" site is coordinated to OH-groups by H-bonds.

3.2. Tobermorite

Quantitative understanding and prediction of the mechanical and chemical properties of hydrated cement paste, including strength, drying shrinkage, creep, and diffusion, requires detailed and fundamental understanding of the behavior of water in nano-confinement and on surfaces of cement paste particles. Computational molecular modeling is an important tool in this effort. The surface areas of hydrated cement pastes are very large, hundreds of m^2/g, and all structural models contain large fractions of nano-porosity [94–97]. Recent ^1H NMR field cycling experiments show substantial amounts of porosity with characteristic dimensions of 5 nm, as well as larger 50 and 500 nm pores (J.-P. Korb, personal communication). These results also yield characteristic pore surface residence times for water molecules of the order of a few μs and correlation times for surface diffusional jumps of about 1 ns [98].

Atomistically detailed MD or MC simulations of complicated systems such as hydrated Ca-silicates require specific input structures, since initial amorphous atomic assemblages of this complexity are not able to explore phase space adequately to find the global minimum-energy structure with available computers. All current molecular scale models of the structure of the C–S–H of hydrated cement paste are based on the layered Ca-silicate structures of tobermorite and jennite, although clearly the C–S–H structure is much more disordered [52,76,77,94–97,99,100]. We present here the first detailed MD calculations of the structure of water on the surface of tobermorite as an initial step in understanding the molecular scale structure and dynamics of water in C–S–H nanopores. Gmira et al. [52] have performed similar calculations focused on understanding the cohesive forces between C–S–H particles and also discuss the limitations of the tobermorite/jennite models.

Our calculations are based on the structure of the 9 Å phase of tobermorite determined by Merlino et al. [101] using single crystal X-ray diffraction methods. The interatomic potentials were those of the *CLAYFF* force field [46]. The simulation model assumes a fully polymerized drierkette chain structure, recognizing that the C–S–H of OPC and even cements with pozzolanic components is less polymerized. The X-ray crystal structure does not specify the positions of the H atoms of Si–OH groups. To have the stoichiometric composition of $Ca_5Si_6O_{16}(OH)_2$, 50% of the non-bridging oxygens (NBOs) need to be Si–O^- and 50% Si–OH. In the simulations, those NBOs pointing outward were assumed to be Si–OH, and those pointing parallel to the layers to be Si–O^- (Fig. 4). Although tobermorite and jennite are thought to contain Si–OH sites [101–105], near infrared spectroscopy of synthetic, tobermorite-type C–S–H shows the absence of the (Si–OH stretching)+(O–H stretching) combination band at 4567 cm^{-1} at Ca/Si ratios greater than to 1.2, indicating the absence of Si–OH linkages at Ca/Si ratios greater than this [77]. Detailed understanding of the protonation state of C–S–H in cement pastes of different types will be essential to molecular modeling of water in C–S–H nano pores and surfaces.

The MD simulations were performed for a cell containing 2×4×2 crystallographic unit cells of 9-Å tobermorite [101] in contact with ~40 Å layer of 0.25 M KCl aqueous solution

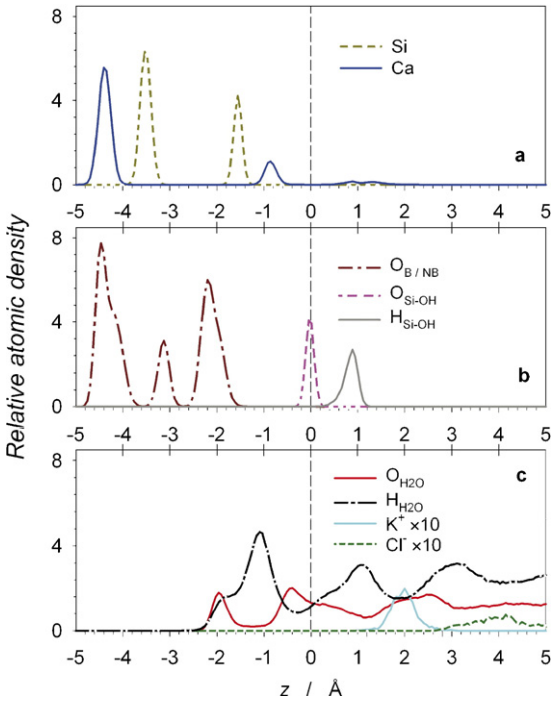

Fig. 5. Computed atomic density profiles for water molecules, Ca^{2+}, K^+, and Cl^- (c) on the surface of 9 Å tobermorite (a,b). The interface ($z=0$) is nominally defined as the average position of the non-bridging oxygens (protonated; pink line) of the bridging silicate tetrahedra. The aqueous layer is located at positive z values, and the tobermorite substrate is located at negative z values, with Si of the bridging tetrahedra occuring at −1.6 Å.

(4 KCl molecules per 882 H_2O molecules). The presence of solute does not significantly affect the behavior of the water molecules at the tobermorite surface. The total number of atoms in the tobermorite interfacial simulation was $N=3646$, and the periodic supercell had dimensions of $22.63\times29.19\times58.18$ Å^3. The MD simulations do an excellent job at reproducing the bulk crystal structure of 9-Å tobermorite using the constant pressure (*NPT*) statistical ensemble. The input structure remains intact during the 200 ps simulation, and the simulated cell dimensions are within 0.5% of the published experimental values [40]. Based on this simulated tobermorite structure, the interfacial simulations are performed in the constant volume (*NVT*) statistical ensemble to allow more efficient analysis of the near-surface fluid structure. As illustrated in Fig. 4, most of the solute K^+ or Cl^- are not strongly associated with the surfaces, but a few of the Ca^{2+} ions from the tobermorite structure that occupy surface sites leave their initial positions and move into the solution.

Detailed analysis of the MD-simulated dynamic trajectory of the system shows that it is possible to effectively distinguish water molecules that spend most of their time within channels between the tetrahedral chains on the tobermorite surface from those that reside above the interface defined by the atomic centers of the exterior non-bridging oxygens of the bridging tetrahedra (vertical dashed lines in Fig. 5). These water molecules are clearly illustrated in the computed atomic density profiles shown in Fig. 5c. Within the channels, there are two sub-layers of water molecules. One has its O_{H_2O} atoms at about the level of the inner non-bridging oxygens (O_{NB}) of the bridging tetrahedra ($z\sim-2.0$ Å in Fig. 5c). The H_{H_2O} shoulder at the same level is due to H-bond donation from the water molecules to these Si–O^- sites. The second water sub-layer in the channels has its O_{H_2O} about 0.4 Å below the level of the O_{SiOH}. The large H_{H_2O} peak at about −1.2 Å is due to H-bond donation from these water molecules to the Si–O^-. There are three sub-layers of O_{H_2O} at about 0.3, 1.8 and 2.6 Å above the level of the O_{SiOH} that constitute the external surface-associated H_2O. The H_{SiOH} (grey peak at ~0.9 Å in Fig. 5b) point outward and donate H-bonds to these H_{H_2O}, which in turn donate H-bonds to each other and to O_{SiOH}. Together, the O_{SiO^-}, O_{SiOH}, H_{SiOH}, O_{H_2O}, and H_{H_2O} form a well-interconnected H-bond network within the channels and across the interface. The H_2O of the two layers in the channel and the closest layer outside the channels also complete the nearest neighbor coordination shell of the Ca ions of the surface (blue peak at −0.85 Å in Fig. 5a). Structuring of the H_{H_2O} and O_{H_2O} by the surface continues to at least 8 Å above the interface (beyond the scale of Fig. 5).

The atomic density maps (Fig. 6) provide a more specific picture of the molecular positions and H-bond structure that confirm the conclusions from the density profiles. Within the channels (Fig. 6a), the water molecules donate H-bonds to both the bridging and non-bridging oxygens of the bridging Si-tetrahedra as well as to other H_2O. Some of the H-bonds exist throughout the 100 ps duration of the simulation, as demonstrated by the dense H-contours, but many others undergo libration (hindered rotations) and even diffusional jumps. The H_2O molecules in the 3 Å thick slice above the nominal interface ($z=0$ in Fig. 5) are more dynamically disordered by librational and diffusional motion than those in the channels, as demonstrated by the more uniform and chaotic O_{H_2O} and H_{H_2O} atomic density

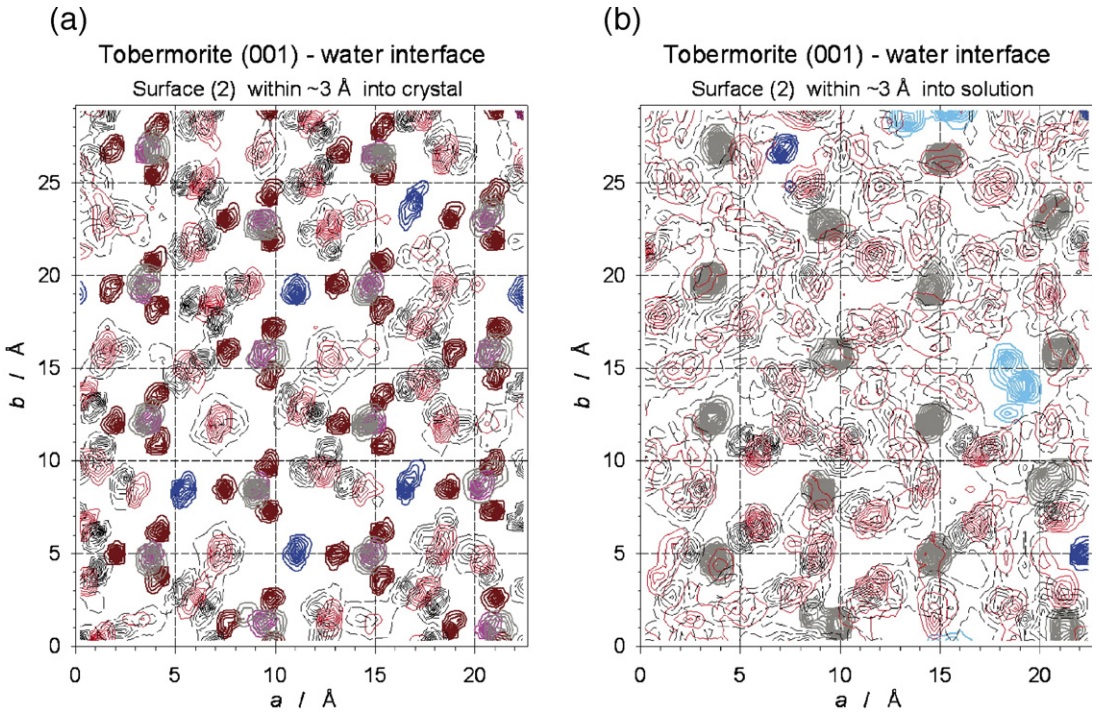

Fig. 6. MD computed atomic density maps on the (001) surface of 9 Å tobermorite. (a) A 3 Å-thick layer into the crystal below the interface (defined as $z=0$ Å in Fig. 5). The drierette silicate chains run top to bottom in this view, with triangles of oxygens (dark red contours) of these tetrahedra clearly visible. Ca^{2+} (dark blue) and H_2O (O — red, H — dashed black) occur in the channels between the tetrahedra. (b) A 3 Å-thick layer above the nominal interface. The H_{SiOH} of the bridging tetrahedra are clearly visible as the dense, ordered grey contours. Occasional Ca^{2+} (dark blue contours) that have diffused out of the channels and K^+ (light blue contours) from the solution are also clearly visible.

contours (red and black contours, respectively; Fig. 6), although those that coordinate Ca ions generally have more stable positions and orientations. The surface Ca ions are somewhat mobile but are mostly confined to the channels and are typically coordinated by three O of the bridging tetrahedra and three or more water molecules. Fig. 6a also illustrates the stable, outward pointing positions of the external Si–OH.

Diffusion coefficients for solution species were calculated from the root-mean-square displacement of the molecules using standard algorithms [64]. The average diffusion coefficients of the surface-associated H_2O molecules that spend most of their time in the channels and those that lie above the nominal interface are significantly different. In the channels $D_{H_2O}=5.0\times10^{-11}$ m^2/s, whereas above the interface $D_{H_2O}=6.0\times10^{-10}$ m^2/s. The average diffusion coefficient for all surface-associated H_2O molecules is about 1.0×10^{-10} m^2/s. All of these values are significantly less than the value of 2.3×10^{-9} m^2/s, characteristic of H_2O molecules in simulations of bulk liquid water using the same force field. As described in the companion paper, these values are in good agreement with the values estimated from ^1H NMR field cycling relaxation experiments [106]. The calculated diffusion coefficients of Ca^{2+} are somewhat less, 3.0×10^{-11} m^2/s in the channels and 5.0×10^{-11} m^2/s if they diffuse above the interface. For those K^+ and Cl^- associated with the surface, the diffusion coefficients (above the interface) are larger, 2.0×10^{-10} m^2/s and 3.8×10^{-10} m^2/s, respectively.

Overall, the MD results here demonstrate that the water at the surface of tobermorite, and by inference those of jennite and C–S–Hs, is highly structured, reflecting the structure, composition and charge distribution of the underlying substrate. For C–S–H, depolymerization of the tetrahedral chains and deprotonation of the non-bridging Si–OHs will likely lead to a significantly different structure and possibly further reduced diffusion coefficients due to H-bonding to $Si–O^-$. For jennite, the near-surface water structure is likely to be somewhat different due to the presence of Ca–OH surface sites on the tilleyite-like ribbons. To the extent that entire sections of drierkette tetrahedral chains are missing from tobermorite-like C–S–H, Ca–OH sites will be important also [77,99,100].

Acknowledgements

This research was supported by DOE Basic Energy Sciences Grant DEFGO2-00ER-15028. Computation was partially supported by the National Computational Science Alliance (Grant EAR 990003N) and utilized NCSA SGI/CRAY Origin 2000 computers and Cerius2-4.9 software package from Accelrys. J. Wang also acknowledges a fellowship from the University of Illinois at Urbana-Champaign. Fruitful discussions with R.T. Cygan about forcefield parameterization are most gratefully acknowledged.

References

[1] K.J. Packer, The dynamics of water in heterogeneous systems, Philos. Trans. R. Soc. Lond., B 278 (1977) 59–87.
[2] J.N. Israelachvili, R.M. Pashley, Molecular laying of water at surfaces and origin of repulsive hydration forces, Nature 306 (1983) 249–250.
[3] M.F. Hochella Jr., A.F. White, Mineral–water interaction geochemistry: an overview, Rev. Miner. 23 (1990) 1–16.
[4] J.N. Israelachvili, H. Wennerström, Role of hydration and water structure in biological and colloidal interactions, Nature 379 (1996) 219–225.
[5] M.I. McCarthy, G.K. Schenter, C.A. Scamehorn, J.B. Nicholas, Structure and dynamics of the water/MgO interface, J. Phys. Chem. 100 (1996) 16989–16995.
[6] C.H. Bridgeman, N.T. Skipper, A Monte Carlo study of water at an uncharged clay surface, J. Phys., Condens. Matter 9 (1997) 4081–4087.
[7] E. Spohr, C. Hartnig, Water in porous glasses. A computer simulations study, J. Mol. Liq. 80 (1999) 165–178.
[8] E. Stöckelmann, R. Hentschke, A molecular-dynamics simulation study of water on NaCl (001) using a polarizable model, J. Chem. Phys. 110 (1999) 12097–12107.
[9] G.E. Brown, V.E. Henrich, W.H. Casey, D.L. Clark, C. Eggleston, A. Felmy, D.W. Goodman, M. Grätzel, G. Maciel, M.I. McCarthy, K.H. Nealson, D.A. Sverjensky, M.F. Toney, J.M. Zachara, Metal oxide surfaces and their interactions with aqueous solutions and microbial organisms, Chem. Rev. 99 (1999) 77–174.
[10] L.J. Criscenti, D.A Sverjensky, The role of electrolyte anions (ClO_4^-, NO_3^-, and Cl^-) in divalent metal (M^{2+}) adsorption on oxide and hydroxide surfaces in salt solutions, Am. J. Sci. 299 (1999) 828–899.
[11] G. Sposito, N.T. Skipper, R. Sutton, S.H. Park, A.K. Soper, J.A. Greathouse, Surface geochemistry of the clay minerals, Proc. Natl. Acad. Sci. U. S. A. 96 (1999) 3358–3364.
[12] A.G. Kalinichev, R.J. Kirkpatrick, R.T. Cygan, Molecular modeling of the structure and dynamics of the interlayer and surface species of mixed-metal layered hydroxides: chloride and water in hydrocalumite (Friedel's salt), Am. Mineral. 85 (2000) 1046–1052.
[13] J. Greathouse, K. Refson, G. Sposito, Molecular dynamics simulations of water mobility in magnesium-smectite hydrates, J. Am. Chem. Soc. 122 (2000) 11459–11464.
[14] J. Dore, Structural studies of water in confined geometry by neutron diffraction, Chem. Phys. 258 (2000) 327–347.
[15] P. Fenter, P. Geissbuhler, E. DiMasi, G. Srajer, L.B. Sorensen, N.C. Sturchio, Surface speciation of calcite observed in situ by high-resolution X-ray reflectivity, Geochim. Cosmochim. Acta 64 (2000) 1221–1228.
[16] P. Fenter, H. Teng, P. Geissbuhler, J.M. Hanchar, K.L. Nagy, N.C. Sturchio, Atomic-scale structure of the orthoclase (001)-water interface measured with high-resolution X-ray reflectivity, Geochim. Cosmochim. Acta 64 (2000) 3663–3673.
[17] N. Nandi, K. Bhattacharyya, B. Bagchi, Dielectric relaxation and salvation dynamics of water in complex chemical and biological systems, Chem. Rev. 100 (2000) 2013–2045.
[18] U. Raviv, P. Laurat, J. Klein, Fluidity of water confined to subnanometre films, Nature 413 (2001) 51–54.
[19] Y. Zhu, S. Granick, Viscosity of interfacial water, Phys. Rev. Lett. 87 (2001) 09614-1-4.
[20] G.E. Brown, Surface science — how minerals react with water, Science 294 (2001) 67–69.
[21] L. Cheng, P. Fenter, K.L. Nagy, M.L. Schlegel, N.C. Sturchio, Molecular-scale density oscillations in water adjacent to a mica surface, Phys. Rev. Lett. (2001) 8715 156103-1-4.
[22] O. Teschke, G. Ceotto, E.F. de Souza, Interfacial aqueous solutions dielectric constant measurements using atomic force microscopy, Chem. Phys. Lett. 326 (2000) 328–334.
[23] M.-C. Bellissent-Funel, Structure of confined water, J. Phys., Condens. Matter 13 (2001) 9165–9177.
[24] M.-C. Bellissent-Funel, Water near hydrophilic surfaces, J. Mol. Liq. 96–97 (2002) 287–304.
[25] L.J. Michot, F. Villiéras, M. Francois, I. Bihannic, M. Pelletier, J.-M. Cases, Water organization at the solid–aqueous solution, C. R., Geosci. 334 (2002) 611–631.
[26] A. Fouzri, R. Dorbez-Sridi, M. Oumezzine, Water confined in silica gel and in vycor glass at low and room temperature, X-ray diffraction study, J. Chem. Phys. 116 (2002) 791–797.
[27] S.-H. Park, G. Sposito, Structure of water adsorbed on a mica surface, Phys. Rev. Lett. 89 (2002) 085501.

[28] H. Sakuma, T. Tsuchiya, K. Kawamura, K. Otsuki, Large self-diffusion of water on brucite surface by ab initio potential energy surface and molecular dynamics simulations, Surf. Sci. 536 (2003) L396–L402.
[29] J.J. Thomas, D.A. Neumann, S.A. FitzGerald, R.A. Livingston, State of water in hydrating tricalcium silicate and portland cement pastes as measured by quasi-elastic neutron scattering, J. Am. Ceram. Soc. 84 (2001) 1811–1816.
[30] A.J. Allen, J.C. McLaughlin, D.A. Neumann, R.A. Livingston, In situ quasi-elastic scattering characterization of particle size effects on the hydration of tricalcium silicate, J. Mater. Res. 19 (2004) 3242–3254.
[31] A. Faraone, E. Fratini, P. Baglioni, Quasieleastic and inelastic neutron scattering on hydrated calcium silicate pastes, J. Chem. Phys. 121 (2004) 3212–3220.
[32] P.J. McDonald, J.P. Korb, J. Mitchell, Surface relaxation and chemical exchange in a hydrating cement pastes: 1 two-dimensional NMR relaxation study, Phys. Rev., E 72 (2005) Art. No. 011409 Part 1.
[33] V.K. Peterson, D.A. Neumann, R.A. Livingston, Hydration of tricalcium and dicalcium silicate mixtures studied using quasielestic neutron scattering, J. Phys. Chem., B 109 (2005) 14449–14453.
[34] S.H. Lee, P.J. Rossky, A comparison of the structure and dynamics of liquid water at hydrophobic and hydrophilic surface—a molecular dynamics simulation study, J. Chem. Phys. 100 (1994) 3334–3345.
[35] B. Hartnig, W. Witschel, E. Spohr, Molecular dynamics study of the structure and dynamics of water in cylindrical pores, J. Phys. Chem. 102 (1998) 1241–1249.
[36] A.G. Kalinichev, Y.E. Gorbaty, A.V. Okhulkov, Structure and H-bonding of liquid water at high hydrostatic pressure: Monte Carlo NPT-ensemble simulations up to 10 kbar, J. Mol. Liq. 82 (1999) 57–72.
[37] M.C. Gordillo, J. Martí, H-bond structure of liquid water confined in nanotubes, Chem. Phys. Lett. 329 (2000) 341–345.
[38] R.T. Cygan, Molecular modeling in mineralogy and geochemistry, Rev. Mineral. Geochem. 42 (2001) 1–36.
[39] P. Gallo, M. Rapinesi, M. Rovere, Confined water in the low hydration regime, J. Chem. Phys. 117 (2002) 369–375.
[40] A.G. Kalinichev, R.J. Kirkpatrick, Molecular dynamics modeling of chloride binding to the surfaces of Ca hydroxide, hydrated Ca-aluminate and Ca-silicate phases, Chem. Mater. 14 (2002) 3539–3549.
[41] J.R. Rustad, A.R. Felmy, E.J. Bylaska, Molecular simulation of the magnetite water interface, Geochim. Cosmochim. Acta 67 (2003) 1001–1016.
[42] J. Wang, A.G. Kalinichev, R.J. Kirkpatrick, Molecular structure of water confined in brucite, Geochim. Cosmochim. Acta 68 (2004) 3351–3365.
[43] M. Odelius, M. Bernasconi, M. Parrinello, Two dimensional ice adsorbed on mica surface, Phys. Rev. Lett. 78 (1997) 2855–2858.
[44] D. Marx, Throwing tetrahedral dice, Science 303 (2004) 634–636.
[45] B. Guillot, A reappraisal of what we have learnt during three decades of computer simulations on water, J. Mol. Liq. 101 (2002) 219–260.
[46] R.T. Cygan, J.J. Liang, A.G. Kalinichev, Molecular models of hydroxide, oxyhydroxide, and clay phases and the development of a general force field, J. Phys. Chem., B 108 (2004) 1255–1266.
[47] R.T. Cygan, J.D. Kubicki (Eds.), Molecular Modeling Theory and Applications in the Geosciences, Reviews in Mineralogy and Geochemistry, vol. 42, Mineralogical Society of America, Washington, D.C., 2001
[48] R.J. Kirkpatrick, A.G. Kalinichev, J. Wang, X. Hou, J.E. Amonette, Molecular modeling of the vibrational spectra of interlayer and surface species of layered double hydroxides, in: J.T. Kloprogge (Ed.), The Application of Vibrational Spectroscopy to Clay Minerals and Layered Double Hydroxides, CMS Workshop Lectures, vol. 13, The Clay Mineral Society, Aurora, CO, USA, 2004, pp. 239–285.
[49] R.J.M. Pellenq, J.M. Caillol, A. Delville, Electrostatic attraction between two charged surfaces: A (N,V,T) Monte Carlo simulation, J. Phys. Chem., B 42 (1997) 8584–8594.
[50] A. Delville, R.J.M. Pellenq, Electrostatic attraction and/or repulsion between charged colloids: A (NVT) Monte-Carlo study, Mol. Simul. 24 (2000) 1–24.
[51] S. Lesko, E. Lesniewska, A. Nonat, Investigation by atomic force microscopy of forces at the origin of cement cohesion, Utramicroscopy 86 (2001) 11–21.
[52] A. Gmira, M. Zabat, R.J.-M. Pellenq, H. Van Damme, Microscopic physical basis of the macroscopic poromechanical behavior of concrete, Mater. Struct. Concr. Sci. Eng. 37 (2004) 3–14.
[53] R.J.M. Pellenq, On the origin of cement cohesion, Actual. Chim. Suppl. 273 (2004) 12–22.
[54] R.J.M. Pellenq, H. van Damme, Why does concrete set?: The nature of cohesion forces in hardened cement-based materials, Mater. Res. Soc. Bull. 29 (2004) 319–323.
[55] B. Jonsson, H. Wennerstrom, A. Nonat, B. Cabane, Onset of cohesion in cement paste, Langmuir 20 (2004) 6702–6709.
[56] B. Jonsson, A. Nonat, C. Labbez, B. Cabane, H. Wennerstrom, Controlling the cohesion of cement paste, Langmuir 21 (2005) 9211–9221.
[57] B. Jonsson, H. Wennerstrom, Ion–ion correlations in liquid dispersions, J. Adhes. 80 (2004) 339–364.
[58] C. Plassard, E. Lesniewska, I. Pochard, A. Nonat, Nanoscale experimental investigation of particle interactions at the origin of the cohesion of cement, Langmuir 21 (2005) 7263–7270.
[59] P. Faucon, J.M. Delaye, J. Virlet, J.F. Jacquinot, F. Adenot, Study of the structural properties of the C–S–H(I) by molecular dynamics simulation, Cem. Concr. Res. 27 (1997) 1581–1590.
[60] I.S. Bell, P.V. Coveney, Molecular modeling of the mechanism of action of borate retarders on hydrating cements at high temperature, Mol. Simul. 20 (1998) 331–356.
[61] P.V. Coveney, W. Humphries, Molecular modelling of the mechanism of action of phosphonate retarders on hydrating cements, J. Chem. Soc., Faraday Trans. 92 (1996) 831–841.
[62] R.J. Kirkpatrick, P. Yu, A.G. Kalinichev, Chloride binding to cement phases: exchange isotherm, ^{35}Cl NMR and molecular dynamics modeling studies, in: J. Skalny (Ed.), Calcium Hydroxide in Concrete, Am. Ceram. Soc., Materials Science of Concrete Special Volume, , 2001, pp. 77–92.
[63] R.J. Kirkpatrick, A.G. Kalinichev, X. Hou, L. Struble, Experimental and molecular dynamics modeling studies of interlayer swelling: water in kanemite and ASR gel, Mater. Struct. Concr. Sci. Eng. 38 (2005) 449–458.
[64] D. Frenkel, B. Smit, Understanding Molecular Simulation: from Algorithms to Applications, 2nd edition, Academic Press, San Diego, 2002 638 pp.
[65] H.J.C. Berendsen, J.P.M. Postma, W.F. van Gunsteren, J. Hermans, Interaction models for water in relation to protein hydration, in: B. Pullman (Ed.), Intermolecular Forces, Riedel, Dordrecht, 1981, pp. 331–342.
[66] O. Teleman, B. Jönsson, S. Engström, A molecular dynamics simulation of a water model with intramolecular degrees of freedom, Mol. Phys. 60 (1987) 193–203.
[67] W.L. Jorgensen, J. Chandrasekhar, J.F. Madura, R.W. Impey, M.L. Klein, Comparison of simple potential functions for simulating liquid water, J. Chem. Phys. 79 (1983) 926–935.
[68] A.G. Kalinichev, Molecular simulations of liquid and supercritical water: Thermodynamics, structure and hydrogen bonding, Rev. Mineral. Geochem. 42 (2001) 83–129.
[69] T. Head-Gordon, G. Hura, Water structure from scattering experiments and simulation, Chem. Rev. 102 (2002) 2651–2670.
[70] J.R. Rustad, Molecular models of surface relaxation, hydroxylation, and surface charging at oxide-water interfaces, Rev. Mineral. Geochem. 42 (2001) 169–197.
[71] A.C.T. van Duin, A. Strachan, S. Stewman, Q. Zhang, X. Xu, W.A. Goddard, ReaxFF SiO: Reactive force field for silicon and silicon oxide systems, J. Phys. Chem., A 107 (2003) 3803–3811.
[72] T. Zhu, J. Li, X. Lin, S. Yip, Stress-dependent molecular pathways of silica-water reaction, J. Mech. Phys. Solids 53 (2005) 1597–1623.
[73] R.J. Kirkpatrick, A.G. Kalinichev, J. Wang, Molecular dynamics modeling of mineral interlayers and surfaces: Structure and dynamics, Mineral. Mag. 69 (2005) 287–306.
[74] A. Luzar, Resolving the H-bond dynamics conundrum, J. Chem. Phys. 113 (2000) 10663–10675.
[75] J. Teixeira, M.-C. Bellissent-Funel, S.-H. Chen, Dynamics of water studied by neutron scattering, J. Phys., Condens. Matter 2 (1990) SA105–SA108.

[76] H.F.W. Taylor, Cement Chemistry, 2nd ed. Thomas Telford Publishing, London, 1997.
[77] P. Yu, R.J. Kirkpatrick, B. Poe, P.F. McMillan, X.-D. Cong, The structure of calcium silicate hydrate (C–S–H): Near-, mid-, and far-infrared spectroscopy, J. Am. Ceram. Soc. 82 (1999) 742–748.
[78] P.S. Braterman, Z.P Xu, F. Yarberry, Chemistry of layered double hydroxides, in: S.A. Auerbach, K.A. Carrado, P.K. Dutta (Eds.), Handbook of Layered Materials, Marcel Dekker, 2004, pp. 373–474.
[79] J. Wang, A.G. Kalinichev, R.J. Kirkpatrick, R.T. Cygan, Structure, energetics, and dynamics of water adsorbed on the muscovite (001) surface: A Molecular dynamics simulation, J. Phys. Chem., B 109 (2005) 15893–15905.
[80] F.F. Abraham, The interfacial density profile of a Lennard-Jones fluid in contact with a (100) Lennard-Jones wall and its relationship to idealized fluid/wall systems: a Monte Carlo simulation, J. Chem. Phys. 68 (1978) 3713–3716.
[81] D. Eisenberg, W. Kauzmann, The Structure and Properties of Water, Oxford University Press, Oxford, 1969 296 pp.
[82] A.K. Soper, The radial distribution functions of water and ice from 220 to 673 K and at pressure up to 400 MPa, Chem. Phys. 258 (2000) 121–137.
[83] J.R. Errington, P.J. Debenedetti, Relationship between structural order and the anomalies of liquid water, Nature 409 (2001) 318–321.
[84] P.-L. Chau, A.J. Hardwick, A new order parameter for tetrahedral configurations, Mol. Phys. 93 (1998) 511–518.
[85] J. Wang, A.G. Kalinichev, R.J. Kirkpatrick, Effects of substrate structure and composition on the structure, dynamics and energetics of water on mineral surfaces: a molecular dynamics modeling study, Geochim. Cosmochim. Acta 70 (2006) 562–582.
[86] A. Geiger, H.U. Stanley, Low-density "patches" in the hydrogen-bond network of liquid water: Evidence from molecular-dynamics computer simulations, Phys. Rev. Lett. 49 (1982) 1749–1752.
[87] A.N. Paulo, F.W. Starr, M.C. Barbosa, H.E. Stanley, Relation between structure and dynamical anomalies in supercooled water, Physica, A 314 (2002) 470–476.
[88] D.C. Rapaport, H-bonds in water: network organization and lifetimes, Mol. Phys. 50 (1983) 1151–1162.
[89] K. Bagchi, S. Balasubramanian, M.L. Klein, The effects of pressure on structure and dynamical properties of associated liquids: molecular dynamics calculations for the extended simple point charge model of water, J. Chem. Phys. 107 (1997) 8561–8567.
[90] A.M. Saitta, F. Datchi, Structure and phase diagram of high density water: The role of interstitial molecules, Phys. Rev., E 67 (2003) 020201.
[91] H. Engelhardt, B. Kamb, Structure of ice IV, a metastable high-pressure phase, J. Chem. Phys. 75 (1981) 5887–5899.
[92] W.F. Kuhs, J.L. Finney, C. Vettier, D.V. Bliss, Structure and hydrogen ordering in ice VI, VII, and VIII by neutron powder diffraction, J. Chem. Phys. 81 (1984) 3612–3623.
[93] E. Schwegler, G. Galli, F. Gygi, Water under pressure, Phys. Rev. Lett. 84 (2000) 2429–2432.
[94] H.M. Jennings, A model for the microstructure of calcium silicate hydrate in cement paste, Cem. Concr. Res. 30 (2000) 101–116.
[95] H.M. Jennings, Colloid model of C–S–H and implication to the problems of creep and shrinkage, Mater. Struct. Concr. Sci. Eng. 37 (2004) 59–70.
[96] I.G. Richardson, The nature of C–S–H in hardened cements, Cem. Concr. Res. 29 (1999) 1131–1147.
[97] I.G. Richardson, Tobermorite/jennite- and tobermorite/calcium hydroxide-based models for the structure of C–S–H: applicability to hardened pastes of tricalcium silicate,-dicalcium silicate, Portland cement, and blends of Portland cement with blast-furnace slag, metakaolin, or silica fume, Cem. Concr. Res. 34 (2004) 1733–1777.
[98] J.-P. Korb, L. Monteilhet, P.J. McDonald, J. Mitchell, Microstructure and texture of hydrated cement-based materials: a proton field-cycling relaxometry approach, Cem. Concr. Res. 37 (2007) 295–302 (this issue), doi:10.1016/j.cemconres.2006.08.002.
[99] X.-D. Cong, R.J. Kirkpatrick, ^{29}Si MAS NMR study of the structure of calcium silicate hydrate, Adv. Cem. Based Mater. 3 (1996) 144–156.
[100] X.-D. Cong, R.J. Kirkpatrick, J.L. Yarger, P.F. McMillan, The structure of calcium silicate hydrate: NMR and Raman spectroscopic results, in: P. Colombet, A.R. Grimmer, H. Zanni, P. Sozzani (Eds.), Nuclear Magnetic Resonance Spectroscopy of Cement Based Materials, Springer-Verlag, Berlin, 1998.
[101] S. Merlino, E. Bonaccorsi, T. Armbruster, The real structures of clinotobermorite and tobermorite 9 Å: OD character, polytypes and structural relationships, Eur. J. Mineral. 12 (2000) 411–429.
[102] S. Merlino, E. Bonaccorsi, T. Armbruster, Tobermorites: their real structures and order–disorder (OD) character, Am. Mineral. 84 (1999) 1613–1621.
[103] S. Merlino, E. Bonaccorsi, T. Armbruster, The real structure of 11 Å tobermorite: normal and anomalous forms, OD character and polytypic modifications, Eur. J. Mineral. 13 (2001) 577–590.
[104] E. Bonaccorsi, S. Merlino, H.F.W. Taylor, The structure of jennite $Ca_9Si_6O_{18}(OH)_6{\cdot}8H_2O$, Cem. Concr. Res. 34 (2004) 1481–1488.
[105] E. Bonaccorsi, S. Merlino, A.R. Kampf, The crystal structure of tobermorite 14 Å (plomberite), a C–S–H phase, J. Am. Ceram. Soc. 88 (2005) 505–512.
[106] J.-P. Korb, P.J. McDonald, L. Monteilhet, A.G. Kalinichev, R.J. Kirkpatrick, Comparison of proton field-cycling relaxometry and molecular dynamics simulations for proton-water surface dynamics in cement-based materials, Cem. Concr. Res. (2006) in print.